Projectilelike fragments from ^{14}N beams at 15, 25, and 35 MeV/nucleon

G. S. F. Stephans,* R. V. F. Janssens, D. G. Kovar, and B. D. Wilkins

Argonne National Laboratory, Argonne, Illinois 60439

(Received 11 August 1986)

Momentum distributions of projectilelike fragments produced in the interaction of 15, 25, and 35 MeV/nucleon ^{14}N beams on targets of ^{12}C, ^{24}Mg, ^{27}Al, ^{48}Ti, and ^{58}Ni have been measured. Widths and centroids of the quasielastic component of the distributions have been extracted for fragments ranging from ^{4}He to ^{13}N. The widths are compared with published data and several theoretical predictions. The Friedman model correctly predicts the charge and isotope dependence of the widths at the highest beam energy. At 15 MeV/nucleon some deviations from the trend of the published data suggest the possibility of a different reaction mechanism for the projectile-target combinations studied in the present work.

I. INTRODUCTION

In reactions induced by heavy ions, the velocity distributions of projectile-like fragments detected near the grazing angle frequently peak at roughly the velocity of the beam. This "quasielastic" or "breakup" peak is found at beam energies ranging from the vicinity of the Coulomb barrier up to relativistic energies. Despite its ubiquitous nature, the experimental evidence suggests that the quasielastic fragments are created by different mechanisms in the different energy regimes. At low energies (< 10 MeV/nucleon), the dominant mechanism is assumed to be a transfer reaction or inelastic excitation followed by sequential decay. This picture is supported by the results of coincidence measurements between projectile-like fragments and light particles,[1,2] although possible examples of direct breakup have been found.[3] At relativistic energies, there appears to be little question that direct projectile fragmentation occurs.[4]

One observable used to probe the reaction mechanism is the momentum distribution of the fragments. Energy spectra near the grazing angle can be used to measure the longitudinal momentum, while angular distributions give information about the transverse momentum. Interest in projectile fragment momentum distributions began with the measurement of fragments from relativistic ^{12}C and ^{16}O beams by Greiner et al.[4] In the decade since then, measurements have been performed using a wide variety of beams at energies ranging from 7 MeV/nucleon to 2.1 GeV/nucleon.[5–17] Several theoretical models have been proposed to explain the data.[18–22] Of particular interest is the region between 10 and 40 MeV/nucleon, across which the longitudinal momentum widths are observed to increase by roughly a factor of 4 before saturating at the values found with relativistic projectiles.

In this article, we present data for ^{14}N beams on a variety of targets at energies that span this transition region. Although some published results exist in this energy range, ours is the first set of data covering the entire region using a consistent combination of beam, targets, and detected fragments. A comparison of our widths with published ones suggests that an additional component is present in our data that was weak or nonexistent in previous studies with different projectiles and heavier targets.

II. EXPERIMENTAL PROCEDURE

Experiments were performed using ^{14}N beams at energies of 15, 25, and 35 MeV/nucleon provided by the superconducting cyclotron at the National Superconducting Cyclotron Laboratory, Michigan State University. Data were taken for targets of ^{12}C, ^{24}Mg, ^{27}Al, ^{48}Ti, and ^{58}Ni. Because evaporation residues from fusion reactions were detected as part of the same work, the targets were relatively thin, typically 250–300 μg/cm^2. Projectilelike fragments were identified using a ΔE-E telescope consisting of a 300 μm thick Si surface-barrier detector backed by a 5 mm thick Li drifted Si detector. All measurements were made at 5° in the lab frame. The Si detectors were calibrated using an ^{241}Am alpha source, a precision pulser, and elastic scattering of the beam from the different targets.

In Fig. 1(a), a scatterplot of ΔE versus total energy is shown for ^{14}N on ^{24}Mg at 25 MeV/nucleon. Particles which stopped in the ΔE detector have been suppressed in the figure. The contours of constant charge have been straightened to produce the scatterplot shown in Fig. 1(b). Projecting the data in Fig. 1(b) onto the Y axis yields the spectrum shown in Fig. 2. The resolution was sufficient to determine both the charge and mass of all projectilelike fragments down to a velocity well below that of the beam.

III. EXPERIMENTAL RESULTS

The energy spectrum of each isotope has been used to extract information about the momentum distribution. Ideally, longitudinal momentum should be obtained from data taken at the grazing angle. Using the tables of Wilcke et al.,[23] one can estimate that the grazing peak will range from about 8° for ^{58}Ni at 15 MeV/nucleon to about 2° for ^{24}Mg at 35 MeV/nucleon. Thus, the single angle setting of 5° is within 3° of the grazing angle for all beam-target combinations. It has been reported that changing the detection angle by 3° results in a 5% change
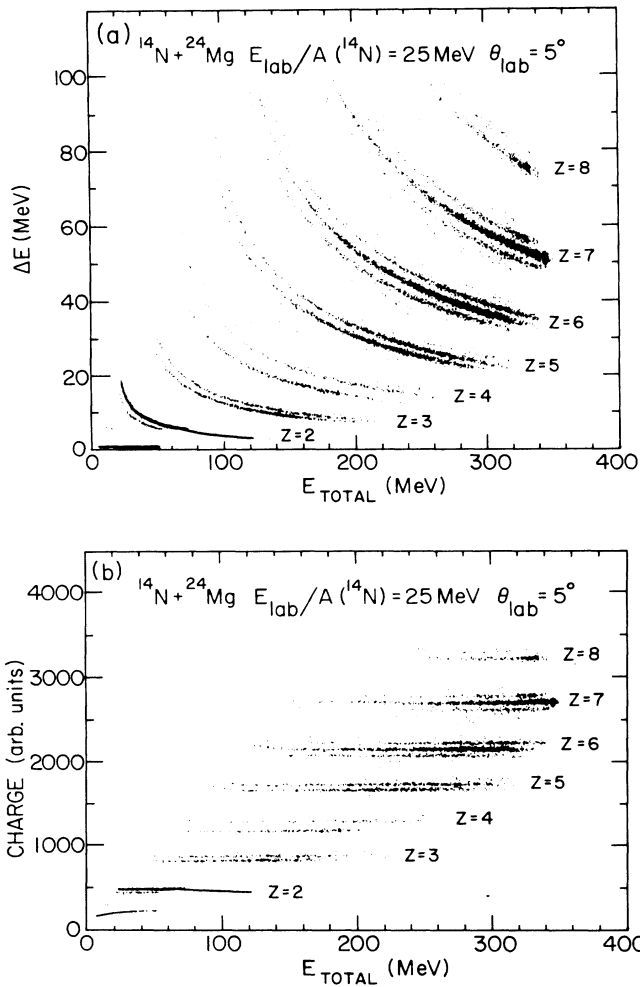

FIG. 2. Projection of the data of Fig. 1(b) onto the y axis, illustrating the mass and charge resolution obtained in the present work.

FIG. 1. (a) Scatterplot of energy in the ΔE detector (in MeV) versus the total energy deposited in the telescope (in MeV). Data are for ^{14}N at 25 MeV/nucleon on a ^{24}Mg target. (b) The contours of constant charge in (a) have been used to calculate a new coordinate proportional to the charge. A scatterplot of this pseudocharge is plotted versus total energy for the same data as shown in (a).

in the width of the observed momentum distribution[12] and the dependence can be reduced even further by careful fitting as described below. Thus, our data should give a fairly reliable indication of the longitudinal momentum distributions.

Figures 3, 4, and 5 show longitudinal momentum spectra in the rest frame of the projectile for ^{12}C, ^{10}B, and ^{7}Be fragments, respectively, at beam energies of 15, 25, and 35 MeV/nucleon. The prominent quasielastic peaks have been fitted with Gaussian curves in order to extract the width. Since it is important to fit only the quasielastic part of the spectrum and not the low-momentum tail, only the data between the high-momentum end and the point on the low-momentum side that is 80% of the maximum were considered, resulting in the lines drawn on the figures. The restrictions used in the fit result in excellent agreement with the slope of the data on the high-energy
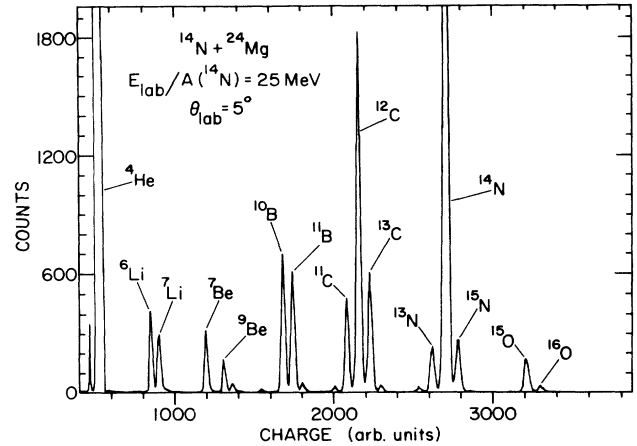
side of the peak, indicating a reasonably good extraction of the width of the quasielastic component.

Momentum widths were extracted for all outgoing isotopes with sufficient statistics for a good fit. The data for ^{4}He and the Li isotopes are questionable at the higher beam energies due to the inability of the telescope to stop the highest energy particles. In agreement with previous work, no significant systematic target dependence was found for the extracted widths. In the following, the values presented are the analysis of those found for all targets. Table I lists the widths extracted for each projectile-like fragment isotope at the three beam energies. The uncertainties in the widths result almost exclusively from the choice of a fitting procedure. The variation due to statistical fluctuations is $\pm 5\%$ or less. As discussed below, a change in the choice of fit limits can result in much larger shifts. For illustration, 10% error bars are shown in Fig. 7.

IV. DISCUSSION

Following the early measurements using relativistic beams,[4] Goldhaber predicted that the longitudinal momentum widths should display a parabolic dependence on the mass of the detected fragment:

$$\sigma^2 = \sigma_0^2 A_f \left[\frac{A_p - A_f}{A_p - 1} \right], \tag{1}$$

where A_f and A_p are the masses of the fragment and projectile, respectively, and σ_0 is a parameter independent of fragment.[18] This mass dependence was found using two independent assumptions. In the statistical model, σ_0 is related to the Fermi momentum of the fragments within the projectile and a value of 100 MeV/c was predicted. The average value found at relativistic energies was about 85 MeV/c. In the equilibrium emission model, σ_0 is related to the temperature. The widths at relativistic energies can be fitted using a temperature of roughly 8.5 MeV. More recently, Bertsch added the influence of Pauli exclusion to the simple statistical model[19] and predicted a
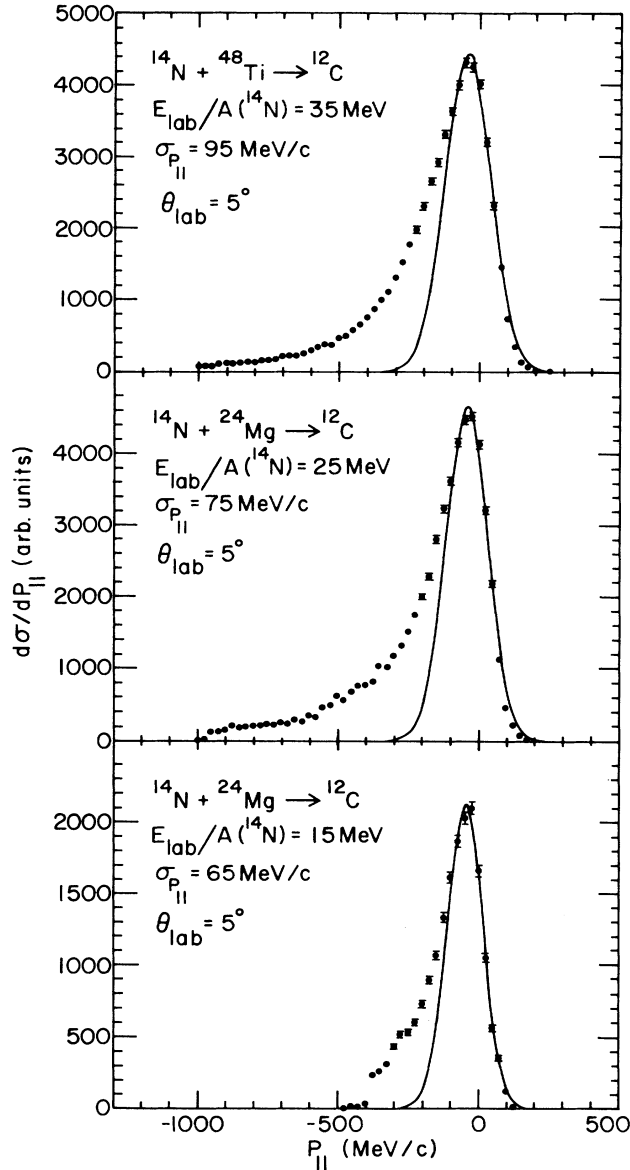
FIG. 3. Longitudinal momentum spectra in the rest frame of the projectile for ^{12}C fragments detected at the three beam energies. The lines are the results of the fit discussed in the text. The widths of the fitted Gaussians are shown for each energy.

FIG. 4. Same as Fig. 3 for ^{10}B fragments.

value for σ_0 which was lower than Goldhaber's initial estimate and thus closer to the experimental value. A further modification by Murphy, which included restrictions on the phase space of the nucleons in the detected fragment, reduces the width even further, so that the prediction of the statistical model is lower than that found experimentally.[22]

Despite these problems with interpretation, the value of σ_0 is a useful quantity to compare different systems since it typically varies by 10—15 % for fragments detected at a given beam energy while the actual widths can vary by as much as a factor of three. Table I lists the values of this parameter for the present data and a comparison to pub-
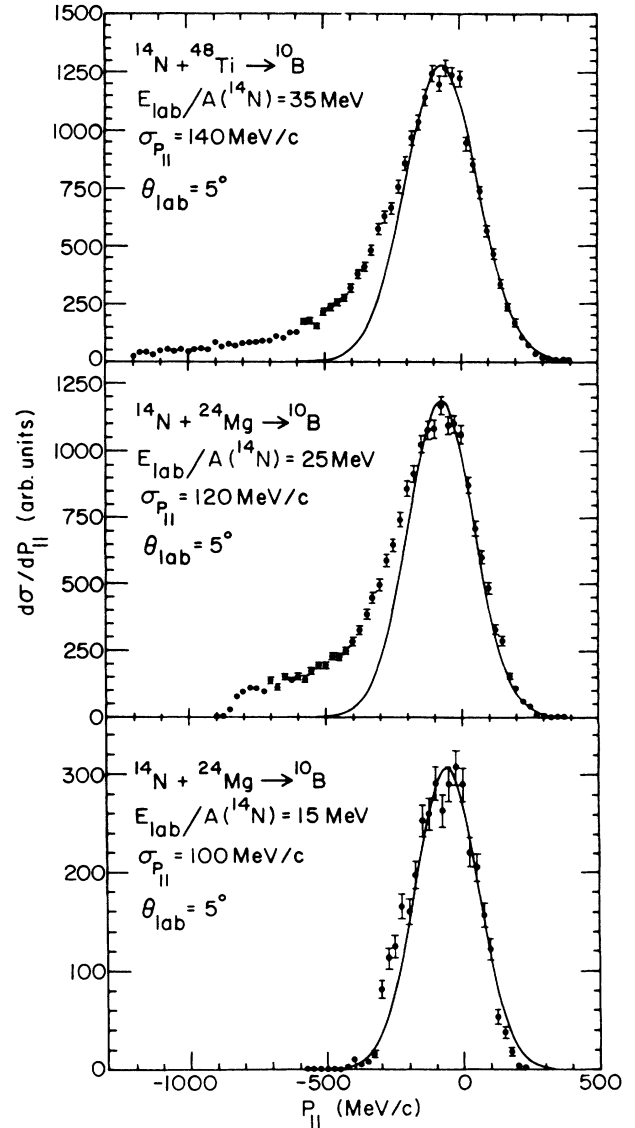
lished results is presented in Fig. 6. For the present work, the widths are labeled by outgoing fragment. Only isotopes detected at all three energies are shown on the figure. Published data have been grouped by projectile. When widths for several detected isotopes were reported, the range of values is indicated by the vertical bars. Published results exist for ^{9}Be at 27.4 MeV/nucleon (Ref. 14); ^{10}B at 32 MeV/nucleon (Ref. 13); ^{12}C at 30 MeV/nucleon (Ref. 12), 86 MeV/nucleon (Ref. 8), and 1.05 GeV/nucleon (Ref. 4); ^{14}N at 30 MeV/nucleon (Ref. 17); ^{16}O at 8.75, 13.6, 15.6, and 19.7 MeV/nucleon (Ref. 11), 92.5 MeV/nucleon (Ref. 7), and 2.1 GeV/nucleon (Ref. 4); ^{20}Ne at 7, 11, 14.5, and 20 MeV/nucleon (Ref. 10), and 43 MeV/nucleon (Ref. 9); and ^{40}Ar at 44 MeV/nucleon (Ref. 16) and 213 MeV/nucleon (Ref. 6). Not shown are the results for ^{40}Ar at 44 MeV/nucleon taken by Borrel et al.,[15] where significantly larger widths than those reported by
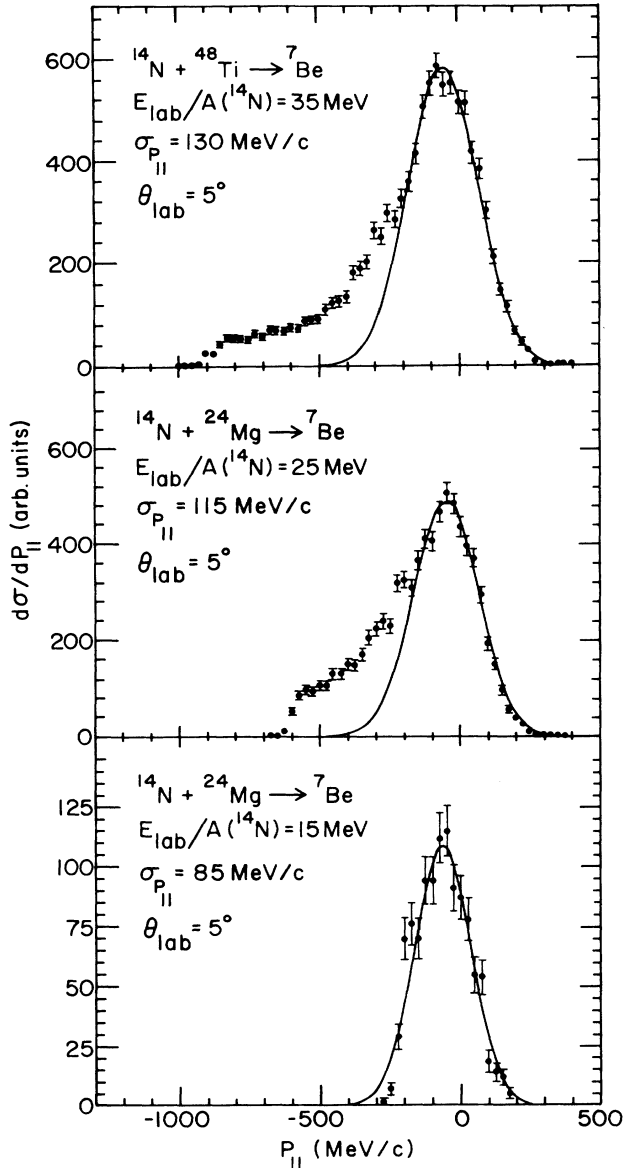
FIG. 5. Same as Fig. 3 for ^{7}Be fragments.

any other group are observed. For the present ^{14}N data, the average value of σ_0, as well as the spread for different isotopes, agrees with published data at 35 MeV/nucleon, but exceeds previously published results at the lower energies. Possible explanations for this discrepancy will be discussed below.

Recently, Friedman has formulated a different model for the fragmentation widths in which the important quantity determining the distribution is the separation energy for the different fragments.[21] Although the parabolic dependence on mass found by Goldhaber does not appear exactly, the widths predicted by this new model do follow roughly the same trend with small variations depending on the isotope. In Fig. 7 the widths predicted with the Friedman model[24] have been converted to a σ_0 value and are compared with the widths found for ^{14}N at 35 MeV/nucleon. The same parameters are used in this calculation as were used for the published calculations for relativistic ^{12}C and ^{16}O. This model correctly predicts the mass dependence of the widths for the C and B isotopes although the relative magnitude between the two Z's is off slightly. The Goldhaber prediction of a constant σ_0 is also shown on the plot for comparison.

The reason for the decrease of the widths with decreasing beam energy remains an unsolved problem. In Friedman's model,[21] Coulomb effects were predicted to reduce the widths, but only by the square root of one minus the ratio of the Coulomb energy divided by the beam energy. For ^{14}N on the heaviest target used in the present work, this term predicts only a 4% decrease in width between 35 and 15 MeV/nucleon, while the data decrease by roughly 35%. A different derivation of Coulomb effects also predicted fairly small effects for the longitudinal width, especially for light projectiles.[20] Since the published data at lower energies are for both projectiles and targets heavier than those used in the present work, some fraction of the discrepancy at 15 MeV/nucleon may be due to Coulomb effects. In the extreme case of Ne on Au, a decrease in width of slightly more than 10% between 35 and 15 MeV/nucleon is predicted by Friedman's model. Thus, existing models would predict only a difference of perhaps 5% between our systems and those for which published data exist.
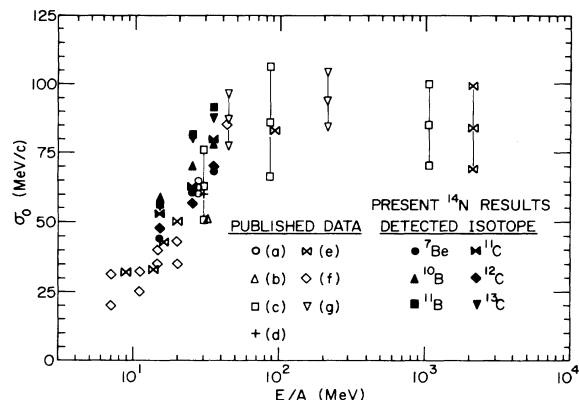
TABLE I. Summary of the momentum width parameters extracted from the present data. See text for discussion.

Fragment	15 MeV/nucleon σ (MeV/c)	15 MeV/nucleon σ_0 (MeV/c)	25 MeV/nucleon σ (MeV/c)	25 MeV/nucleon σ_0 (MeV/c)	35 MeV/nucleon σ (MeV/c)	35 MeV/nucleon σ_0 (MeV/c)
^{4}He	95.8	54.6				
^{6}Li	110.8	57.7	(117.7)	(61.3)		
^{7}Li	119.9	61.8	(132.1)	(68.0)		
^{7}Be	85.5	44.0	117.4	60.5	132.6	68.3
^{10}B	102.2	58.3	123.1	70.2	138.0	78.7
^{11}B	90.0	56.5	129.9	81.5	145.7	91.4
^{11}C	84.1	52.8	100.4	63.0	126.7	79.5
^{12}C	64.5	47.5	77.0	56.7	95.1	70.0
^{13}C	55.9	55.9	80.3	80.3	87.5	87.5
^{13}N			65.1	65.1	99.5	99.5
^{15}N	12.5		12.9		11.9	
^{15}O	14.3		13.8		(8.5)	

FIG. 6. Comparison of the width parameters extracted from the present data with those found for other systems. Published data are for (a) ^{9}Be, (b) ^{10}B, (c) ^{12}C, (d) ^{14}N, (e) ^{16}O, (f) ^{20}Ne, and (g) ^{40}Ar. See text for discussion and references.

A much more likely explanation of the decrease of the widths with energy is a change in the dominant mechanism from direct projectile fragmentation to reactions involving processes such as transfer, perhaps followed by particle evaporation. The existence of processes other than fragmentation is clearly demonstrated by the ^{15}N, ^{15}O, and ^{16}O peaks displayed in Fig. 2. Without angular distributions, it is not possible to extract cross sections for the different isotopes. However, if the ratio of ^{15}O (one proton pickup) to ^{13}C (one proton stripping) is taken as a qualitative measure of the importance of non-fragmentation processes, an increase of approximately 55% occurs between 35 and 15 MeV/nucleon. The effect of this "transfer" component can be seen by comparing the widths for ^{15}N and ^{15}O in Table I to those for the lighter isotopes. The widths of the isotopes heavier than the projectile are roughly constant with energy and are considerably smaller than those for the lighter fragments.

One point must be considered before drawing significant conclusions from this discrepancy. As discussed above, single angle measurements may be misleading. With the present data, it is impossible to eliminate the
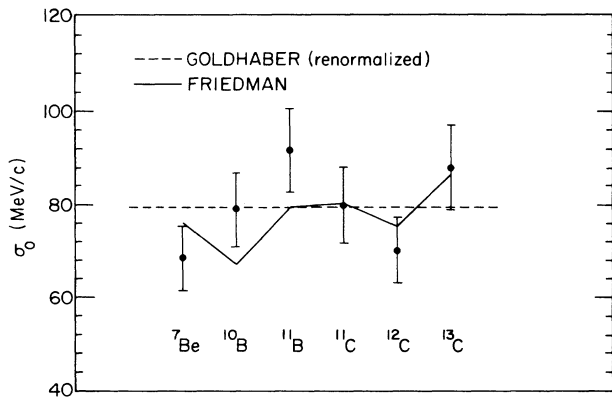

FIG. 7. Comparison of width parameters found in the present work with those found using the models of Goldhaber and Friedman. See text for discussion and references.
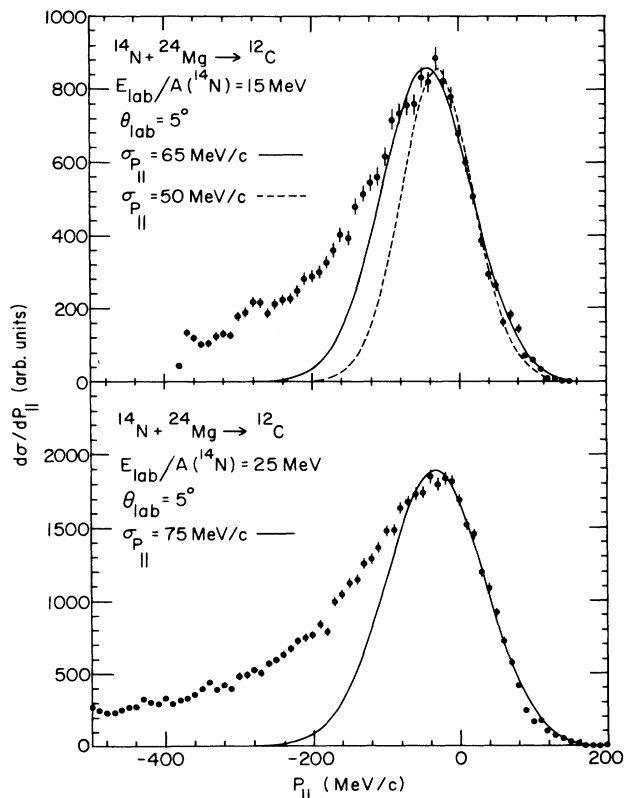

FIG. 8. Same as Fig. 3, except the data are replotted using smaller momentum bins. See text for discussion.

possibility that the data are skewed by the choice of angle, although the agreement of the different targets (each of which will have a different grazing angle) makes it difficult to attribute the difference to failure to measure exactly at the grazing angle for a particular beam-target combination.

Further evidence that an additional component is responsible for the broader widths observed in the present measurements is illustrated in Fig. 8(a), which shows the same data as Fig. 3, except with smaller momentum bins. At 15 MeV, there is evidence for a narrow peak at high momentum with a shoulder. Fitting this narrow structure as shown by the dashed line in Fig. 8(a) gives a value of σ_0 which is closer to that found for ^{16}O on ^{208}Pb (Ref. 11) and ^{20}Ne on ^{197}Au (Ref. 10). For comparison, the spectrum at 25 MeV/nucleon is also shown at the same scale in Fig. 8(b). While there is not clear evidence for a narrow peak with a close shoulder, the possibility of a narrow component cannot be ruled out. The separation of the two components corresponds to a ^{12}C energy difference of between 5 and 10 MeV in the 15 MeV/nucleon spectrum. There is some suggestion of similar substructure in the spectra of other isotopes, but the statistics are poor when the data are binned in such small increments. Also, the total width of the quasielastic peak is the smallest for ^{12}C, making fine features more apparent. The possibility of a shoulder in the beam energy can be rejected based on the energy spectra for elastically scattered ^{14}N particles. Ex-

amination of the energy spectra for the ^{20}Ne + ^{197}Au reactions[10] reveals that the fitted peak shapes used to obtain the published widths follow the data points to a quite low level on the low energy side. Thus, it appears likely that the low energy component was not present in that data, with the result that the reported widths were narrower. Alternatively, the lower momentum component may have been sufficiently weak at the angles used to extract the published widths that it did not affect the results. Within the statistics of the present measurement, the ^{12}C momentum peak shape was the same for the range of targets used at 15 MeV/nucleon (^{12}C to ^{48}Ti).

The exact location of the centroid of the quasielastic peak has received somewhat less attention in the literature than the width. This may be partly due to additional experimental problems. As can be seen in Figs. 3—5, the shift of the quasielastic peak from beam velocity is very small. The fitting ambiguities associated with the large low-energy tail affect the centroid even more strongly than the width. In addition, small inaccuracies in the energy calibration have almost no effect on the width, but can cause large shifts in the extracted centroid energy.

In spite of the problems, several general trends are apparent in the data. As suggested by Figs. 3—5, the velocity of the fragments is almost always less than that of the beam. This is indicative of an inelastic interaction (transferring some of the kinetic energy of the beam into internal excitation) followed by sequential decay. For inelastic excitation followed by sequential decay, the centroid of the velocity of the fragment will be roughly the same as the velocity of the beam following the scattering. Thus, the projectile excitation energy can be estimated from the fragment velocities. In all cases measured in the present work, the implied excitation energy is less than the binary breakup Q value of ^{14}N yielding the observed fragment. Thus, simple sequential breakup of the beam would appear to be ruled out as the sole source for the observed fragments. However, transfer reactions followed by evaporation or breakup cannot be ruled out. Given the quality of the data and the fact that measurements were performed at only one angle, it is not possible to speculate

further about reactions with more complicated kinematics.

Several conclusions can be drawn from the present work. Our measurements of ^{14}N fragmentation reactions support the existence of a gradual transition in the reaction mechanism occurring between roughly 10 and 40 MeV/nucleon. They illustrate the importance of covering a wide energy range with a consistent set of target, projectile, and detected isotopes. The difficulties encountered in analyzing the 15 MeV/nucleon data dramatically demonstrate the fact that simply reporting widths without explicit details about the fitting procedures can result in misleading conclusions. Some evidence was found at 15 MeV/nucleon for a component close in momentum to the quasielastic peak which may not have been present in reactions using other projectiles on heavier targets. Clearly, better data including measurements at more angles for both light and heavy targets would assist in clarifying this possible difference. Coincidence measurements between light particles and projectilelike fragments could resolve this question.

It is interesting to note that heavy-ion fusion reactions also undergo a transition in the energy range between 10 and 40 MeV/nucleon. Below this region, complete fusion of projectile and target is the dominant mechanism. As the beam energy rises, the data suggest that reactions in which only part of the projectile and target fuse become increasingly important, with complete fusion being almost totally nonexistent by about 35 MeV/nucleon.[25] The usual explanation is that the projectile breaks up at some early stage in the reaction and only part of it is captured by the target. One can speculate that the similar range in beam energy for the transition in fusion and fragmentation reaction mechanisms is not a coincidence. Improved data for beam-velocity light particles might help to explain the mechanism of fusion as well as fragmentation in this important energy regime.

*Present address: Massachusetts Institute of Technology, Cambridge, MA 02139.

[1]H. Homeyer et al., Phys. Rev. C 26, 1335 (1982).

[2]P. B. Goldhoorn et al., Phys. Lett. 142B, 14 (1984).

[3]A. C. Shotter, A. N. Bice, J. M. Wouters, W. D. Rae, and J. Cerny, Phys. Rev. Lett. 46, 12 (1981).

[4]D. E. Greiner, P. J. Lindstrom, H. H. Heckman, B. Cork, and F. S. Bieser, Phys. Rev. Lett. 35, 152 (1975).

[5]C. K. Gelbke et al., Phys. Lett. 70B, 415, (1977).

[6]Y. P. Viyogi et al., Phys. Rev. Lett. 42, 33 (1979).

[7]K. Van Bibber et al., Phys. Rev. Lett. 43, 840 (1979).

[8]J. Mougey et al., Phys. Lett. 105B, 25 (1981).

[9]J. B. Natowitz et al., Phys. Rev. Lett. 47, 1114 (1981).

[10]C. Egelhaaf, G. Bohlen, H. Fuchs, A. Gamp, H. Homeyer, and H. Kluge, Phys. Rev. Lett. 46, 813 (1981).

[11]B. G. Harvey, Phys. Rev. Lett. 47, 454 (1981).

[12]A. Menchaca-Rocha et al., Phys. Lett. 131B, 31 (1983).

[13]M. N. Namboodiri et al., Phys. Rev. C 28, 460 (1983).

[14]M. Murphy and R. Stokstad, Phys. Rev. C 28, 428, (1983).

[15]V. Borrel, D. Guerrea, J. Galin, B. Gatty, D. Jacquet, and X. Tarrago, Z. Phys. A 314, 191 (1983).

[16]J. Barrette et al., in Proceedings of the XXIInd International Meeting on Nuclear Physics, Bormio, 1984; R. Dayras, Nucl. Phys. A460, 299 (1986).

[17]D. Guinet, R. Billerey, C. Cerruti, S. Chiodelli, and A. Demeyer, Phys. Lett. 137B, 318 (1984).

[18]A. S. Goldhaber, Phys. Lett. 53B, 306 (1974).

[19]G. Bertsch, Phys. Rev. Lett. 46, 472 (1981).

[20]C. Y. Wong and K. Van Bibber, Phys. Rev. C 25, 2990 (1982).

[21]W. Friedman, Phys. Rev. C 27, 569 (1983).

[22]M. J. Murphy, Phys. Lett. 135B, 25 (1984).

[23]W. W. Wilcke et al., At. Data Nucl. Data Tables 25, 389 (1980).

[24]W. Friedman, private communication.

[25]H. Morgenstern, W. Bohne, W. Galster, K. Grabisch, and A. Kyanowski, Phys. Rev. Lett. 52, 1104 (1984).